N75 28832

SOFT X-RAY DETECTION WITH THE FAIRCHILD 100×100 CCD

George Renda and John L. Lowrance
Princeton University Observatory
Princeton, New Jersey

Princeton has measured the soft x-ray sensitivity of the Fairchild 100×100 element CCD for possible use as a detector in plasma physics research. This paper will explain the experimental setup and the laboratory results. The paper will also present data on slow-scan operation of the CCD and performance when cooled. Results from digital computer processing of the data to correct for element-to-element nonuniformities will also be discussed.

I. INTRODUCTION

Plasma physics research related to nuclear fusion is becoming increasingly interested in diagnostic measurements in the 1-Å to 500-Å spectral region. This region is also of interest in astrophysics. There is particular interest in the CCD type of detector because the intense magnetic fields associated with plasma containment in nuclear fusion research make it awkward, if not impossible, to use more conventional television type image sensors. We have begun a program to measure the soft x-ray sensitivity of CCD image sensors. This paper reports our initial results with the Fairchild 100×100 element CCD. Results from digital computer processing of the video to correct for element-to-element nonuniformities are also discussed. It should be noted that the video signal in this case was obtained with the CCD illuminated with visible wavelength light. The results from computer processing of the x-ray video will be reported in a later paper.

II. SLOW-SCAN, VISIBLE LIGHT PERFORMANCE

A. Test Setup and Tests

Uniform illumination tests were conducted to ascertain the noise characteristics of the CCD with computer processing. Figure 1 shows the test arrangement consisting of the CCD and associated electronics, LED light source, cold chamber, A/D converter and digital tape recorder.

To eliminate dark current and dark current nonuniformities, the CCD was operated at -80°C. The uniform illumination tests covered a range of approximately 60,000 electrons/pixel to 600,000 electrons/pixel, which corresponds to 10 to 100% of full scale for the CCD. The tests were conducted at a pixel clock rate of 5.2 kHz, which resulted in a frame rate of approximately 0.5 frames/sec. The period of integration was varied from 2 seconds to 20 seconds. The LED light source was controlled by a current regulator preset at one specific level.

As a result of the testing, it was found that the predominant noise was coherent. This coherent noise was assumed to be caused by the gain variations in the silicon detectors and charge transfer inefficiency.

The straight line equation ax + b seems to adequately fit the individual pixel data. The "a" term corresponds to the gain or sensitivity of each pixel, and the "b" term corresponds to an initial "zero exposure" offset. This model was assumed, and a computer program was written to find the a's and b's of each pixel element. This full frame set of a's and b's was then used to process other data files.

B. Data Processing

In order to solve for the a and b values of the individual pixels, it is necessary to have two uniform field exposures. As indicated above, the photo-response equation for each pixel is taken to be

$$Y_k = a_n X + b_n \tag{1}$$

where Y_k represents the total number of signal electrons measured at pixel n in file k.

X is used as a scaling factor. For this specific program, X is chosen such that full scale equals 10,000 counts. For example, if Y_k represents, on the average, 25% of full scale, then X is set equal to 2500.

The equation for the second file is

$$Y_{k2} = Na_n X + b_n \tag{2}$$

where Y_{k2} represents the signal measured at pixel n in file k2, and N represents the increase in exposure over Y_k.

The following equations show the steps the computer program goes through to solve for the value of a and b:

$$a_n^X = \frac{Y_{k2} - Y_k}{N - 1} \tag{3}$$

where N - 1 is a data input card to the program; i. e., if Y_{k2} is 4 times greater than Y_k, then N - 1 = 3.

$$a_n = \frac{a_n^X}{X} \tag{4}$$

and

$$b_n = Y_k - a_n^X \tag{5}$$

The values of a_n and b_n for every pixel are then stored as a file on tape. We now have a calibration matrix for the entire CCD array.

The next step is to use these values to remove the coherent noise in a data file of interest.

$$Y_p = \frac{Y_r - b_n}{a_n} \tag{6}$$

where Y_r is the raw (unprocessed) data file of interest and Y_p is the processed data file.

C. Standard Deviation in Computer Processed Data

The following is the general equation for the variance of a sum:

If

$$A = a_1 + a_2$$

then

$$\sigma_A^2 = \sigma_1^2 + \sigma_2^2 \tag{7}$$

and the general equation for the variance of a product is (Ref. 1)

$$A = c_1 a_1^m a_2^n a_3^r \ldots \tag{8}$$

$$\left(\frac{\sigma}{A}\right)^2 = \left(\frac{m\sigma_1}{a_1}\right)^2 + \left(\frac{n\sigma_2}{a_2}\right)^2 + \left(\frac{r\sigma_3}{a_3}\right)^2 \ldots \tag{9}$$

Rewriting Equation (6) in terms of the data used to develop the calibration coefficients a and b,

$$Y_p = \frac{Y_r - b_n}{a_n} = X\left(\frac{(N - 1)\left(Y_r - Y_k\right)}{Y_{k2} - Y_k} + 1\right) \tag{10}$$

and, making the following substitutions,

$$C_1 = X(N - 1) \qquad a_2 = Y_{k2} - Y_k$$

$$m = 1 \qquad \sigma_1^2 = \sigma_r^2 + \sigma_k^2$$

$$n = -1$$

$$a_1 = Y_r - Y_k \qquad \sigma_2^2 = \sigma_{k2}^2 + \sigma_k^2$$

one obtains from Equation (9)

$$\sigma_p = \frac{X\,(N-1)}{Y_{k2} - Y_k}\left(\sigma_r^2 + \sigma_k^2 + \frac{\left(Y_r - Y_k\right)^2\left(\sigma_{k2}^2 + \sigma_k^2\right)}{\left(Y_{k2} - Y_k\right)^2}\right)^{1/2} \tag{11}$$

which has the general form

$$\sigma_p = C_1\left(\sigma_r^2 + \sigma_k^2 + C_2\left(\sigma_{k2}^2 + \sigma_k^2\right)\right)^{1/2}$$

The signal-to-noise ratio is

$$S/N = \frac{Y_p}{\sigma_p} = \frac{\left(Y_r - Y_k + \frac{Y_{k2} - Y_k}{N-1}\right)}{\left(\sigma_r^2 + \sigma_k^2 + \frac{\left(Y_r - Y\right)^2\left(\sigma_{k2}^2 + \sigma_k^2\right)}{\left(Y_{k2} - Y_k\right)^2}\right)^{1/2}} \tag{12}$$

This ratio can be written in a simplified form. Since $Y_{k2} \approx NY_k$, then

$$S/N = \frac{Y_r}{\left(\frac{\sigma_r^2 + \sigma_k^2 + \left(Y_r - Y_k\right)^2\left(\sigma_{k2}^2 + \sigma_k^2\right)}{\left(Y_{k2} - Y_k\right)^2}\right)^{1/2}} \tag{13}$$

D. Experimental Data for Visible Illumination

Figure 2a shows the raw unprocessed video signal for one 100-pixel line at an exposure of 24% of full scale. Figure 2b shows the same line after computer processing. Figures 2c and 2d show the same type of data for an exposure that is 84% of full scale (saturation).

For a more quantitative comparison, the standard deviation was computed over a 50 × 50 pixel patch near the center of the 100 × 100 array.

Table 1 shows the improvement in signal-to-noise ratio after point-by-point calibration of the data. This is compared with the signal-to-noise ratio that one would calculate from Equation (13), assuming that the noise is gaussian; i.e., σ = (number of electrons)$^{1/2}$. The predicted signal-to-noise calculation also includes a readout noise factor of 200 electrons rms per pixel. The actual readout noise characteristics are still under investigation.

Table 1. S/N characteristics (50 × 50 pixel area)

Exposure level, % full scale	S/N raw data	S/N processed data	S/N predicted from Eq. (13)	Ideal, (photoelectrons)$^{1/2}$
24	62	195	236	380
84	71	313	446	710

The standard deviation was also calculated for the 100 pixels along a single line. These results are shown in Table 2.

Table 2. S/N characteristics (100 pixel line)

Exposure level, % full scale	S/N raw data	S/N processed data	S/N predicted from Eq. (13)	Ideal, (photoelectrons)$^{1/2}$
24	62	207	236	380
84	116	438	446	710

The discrepancy between Table 1 and Table 2 for the 84% file may be due to a small number of pixels in the 50 × 50 pixel patch that were several sigmas away from the mean.

The processed data S/N is remarkably close to the predicted S/N in Table 2. Therefore, the assumption of (photoelectron)$^{1/2}$ noise is valid.

This implies that by averaging calibration data frames to achieve higher S/N in the calibration frames, one can closely approach the ideal case. This makes the CCD uniquely attractive for low-contrast applications, such as imagery of solar granulation.

III. SOFT X-RAY DETECTION

In nuclear fusion research, it is important to measure the impurities in the plasma and the total energy being radiated. The sensitivity of silicon over a broad spectral range makes it very attractive, and when configured as a CCD, it is even more attractive because of its relative insensitivity to strong magnetic fields associated with plasma containment. The Fairchild CCD-201 has been illuminated with x-rays from a copper target to explore its applicability for x-ray imagery. A block diagram of the experiment for the x-ray sensitivity measurements is shown in Figure 3.

A. Fairchild CCD-201

The photosensitive area of the CCD-201 is covered by about 1.5 microns of silicon and silicon dioxide that is "dead" in terms of visible radiation. That is, photons absorbed in this layer do not contribute to the signal. The shift registers are covered by an additional layer of aluminum 1.2 microns thick that is opaque to visible radiation. Figure 4 shows the transmission characteristics of the aluminum and silicon layers in the soft x-ray spectral region. As can be seen by the aluminum transmission characteristics, the shift register circuits behind the aluminum are sensitive to the x-ray photons. We have found that the problem of the photosensitive shift register can be circumvented by rapid scanning of the shift registers during the exposure time. One would expect that x-ray exposure of the shift register regions may cause permanent damage as well, but this has not been investigated. With regard to this problem, a back illuminated device would be much better. A back illuminated device would also allow a thinner dead layer, with corresponding improvement in long-wavelength response.

B. X-Ray Data

The equation for the continuous x-ray intensity per unit energy interval is (Ref. 2)

$$I_E = K_1 Z \left(E_o - E\right) + K_2 Z^2 \tag{14}$$

For light elements, the Z^2 term can be neglected, since typically $K_2/K_1 = 0.0025$. N_E, the number of photons per unit energy interval, can be written

$$N_E = KZ \frac{\left(E_o - E\right)}{E} \tag{15}$$

where

- E_o is the high energy limit of the spectrum (eV)
- E is any energy between E_o and 0 (eV)
- Z is the atomic number of the element
- K is the continuous x-ray efficiency constant of the element $\left(eV^{-1}\right)$.

In the case of the CCD, the x-rays are attenuated by the beryllium filter and by the polysilicon and silicon dioxide layers on the CCD. From Figure 4, one notes that the transmission is a function of E. The equation for the number of x-rays per unit energy interval reaching the active silicon is

$$N_{EI} = KZ \frac{E_o - E}{E} \exp\left(-u_1 x_1 E^{-Y_1}\right) \exp\left(-u_2 x_2 E^{-Y_2}\right) \tag{16}$$

where $\exp\left(-u_1 x_1 E^{-Y_1}\right)$ is the transmission function for the beryllium, and the silicon transmission is expressed by a similar term.

The silicon has a conversion efficiency of one electron-hole pair per 3.5 electron volts of energy. The number of photoelectrons per unit energy is then

$$N_{pe} = KZ \frac{E_o - E}{3.5} \exp\left(-u_1 x_1 E^{-Y_1}\right) \exp\left(-u_2 x_2 E^{-Y_2}\right) \tag{17}$$

And for a given electron accelerating voltage E_o, the response of the CCD is

$$\sum_{o}^{E_o} N_{pe} = \frac{KZ}{(3.5)(4\pi)} \int_o^{E_o} \left(E_o - E\right) \exp\left(-u_1 x_1 E^{-Y_1}\right) \exp\left(-u_2 x_2 E^{-Y_2}\right) dE$$

photoelectrons steradian^{-1} electron^{-1} (18)

The characteristic x-ray spectra of interest are the L shell lines $L_{\alpha 1,2}$ and $L_{\beta 1}$ at 0.928 and 0.948 keV, respectively. The other L series lines are either weak compared to these lines or are sufficiently attenuated by the beryllium filter so that they are negligible in these measurements.

The empirically derived equation (Ref. 3)

$$N = n\left(E_o - E^*\right)^{1.63} \text{ photons electron}^{-1} \qquad (19)$$

gives the characteristic line strength, where E^* is the line of interest (keV) and n is the efficiency coefficient. Efficiency coefficients for $L_{\alpha 1,2}$ are published for heavier elements and have been extrapolated to yield a value of 3.4×10^{-5} for copper. The ratio of $L_{\alpha 1,2}$ to $L_{\beta 1}$ is 2. Therefore, the combined characteristic line strength is given by the equation

$$N = \frac{3.4 \times 10^{-5}}{3.5 \times 4\pi} \left(K_\alpha \left(E_o - E_{L_{\alpha 1,2}}\right)^{1.63} E_{L_{\alpha 1,2}} + \frac{K_\beta}{2}\left(E_o - E_{L_{\beta 1}}\right)^{1.63} E_{L_{\beta 1}} \right)$$

photoelectrons steradian^{-1} electron^{-1} (20)

where K_α and K_β are the attenuation factors for the filter and dead layer at the characteristic line energy.

Figure 5 shows the sum of Equations (18) and (20) plotted as a solid line and the experimental results plotted as points. There is a close agreement between the experimental data and the calculated response from 1.7 to 6 keV.

The rolloff in response at lower energies is readily attributed to a somewhat thicker beryllium filter and/or thicker layers of polysilicon and silicon dioxide on the CCD.

The actual CCD signal current, when converted to photoelectrons in the silicon per steradian per incident electron on the x-ray target, agrees with the calculated value when one uses a value for the continuous x-ray efficiency constant K/2 of 1.3×10^{-9} eV^{-1} and an active CCD area of 7 mm^2 out of a total area of 12 mm^2.

ACKNOWLEDGEMENTS

The authors wish to thank Edward Loh and Patrick Murray for their aid in obtaining the experimental data, and Paul Zucchino for assistance in the data analysis. We also wish to thank Dr. Martin Green for his assistance in understanding the characteristic x-ray production efficiency. This work was supported by the Energy Research Administration.

REFERENCES

1. L. Tuttle and J. Satterly, The Theory of Measurements, Longmans, Green and Co., London, pp. 215-220 (1925).
2. N. A. Dyson, X-rays in Atomic and Nuclear Physics, Longman Group Limited, London, pp. 7-61 (1973).
3. M. Green and V. E. Cosslett, Brit. J. Appl. Phys. (J. Phys. D.), 1, 425 (1968).

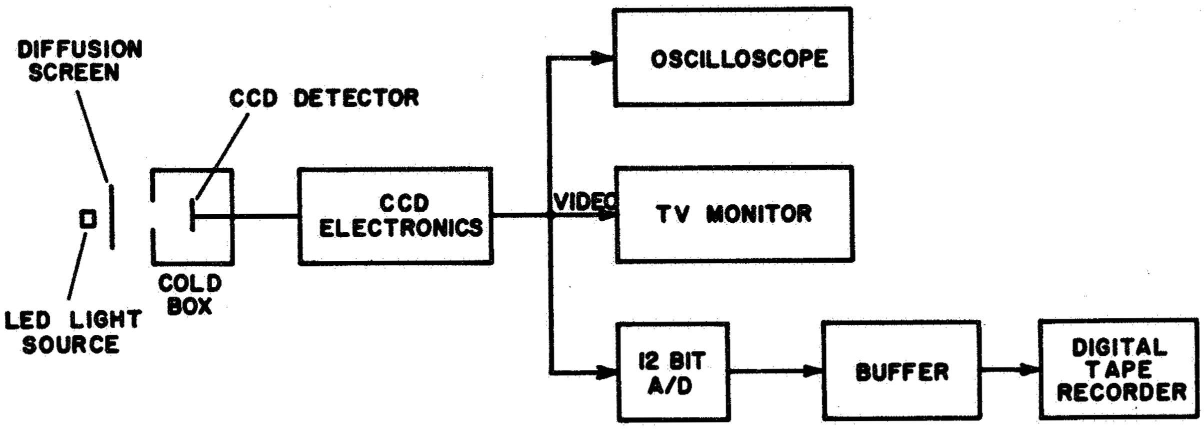

Figure 1. CCD test block diagram

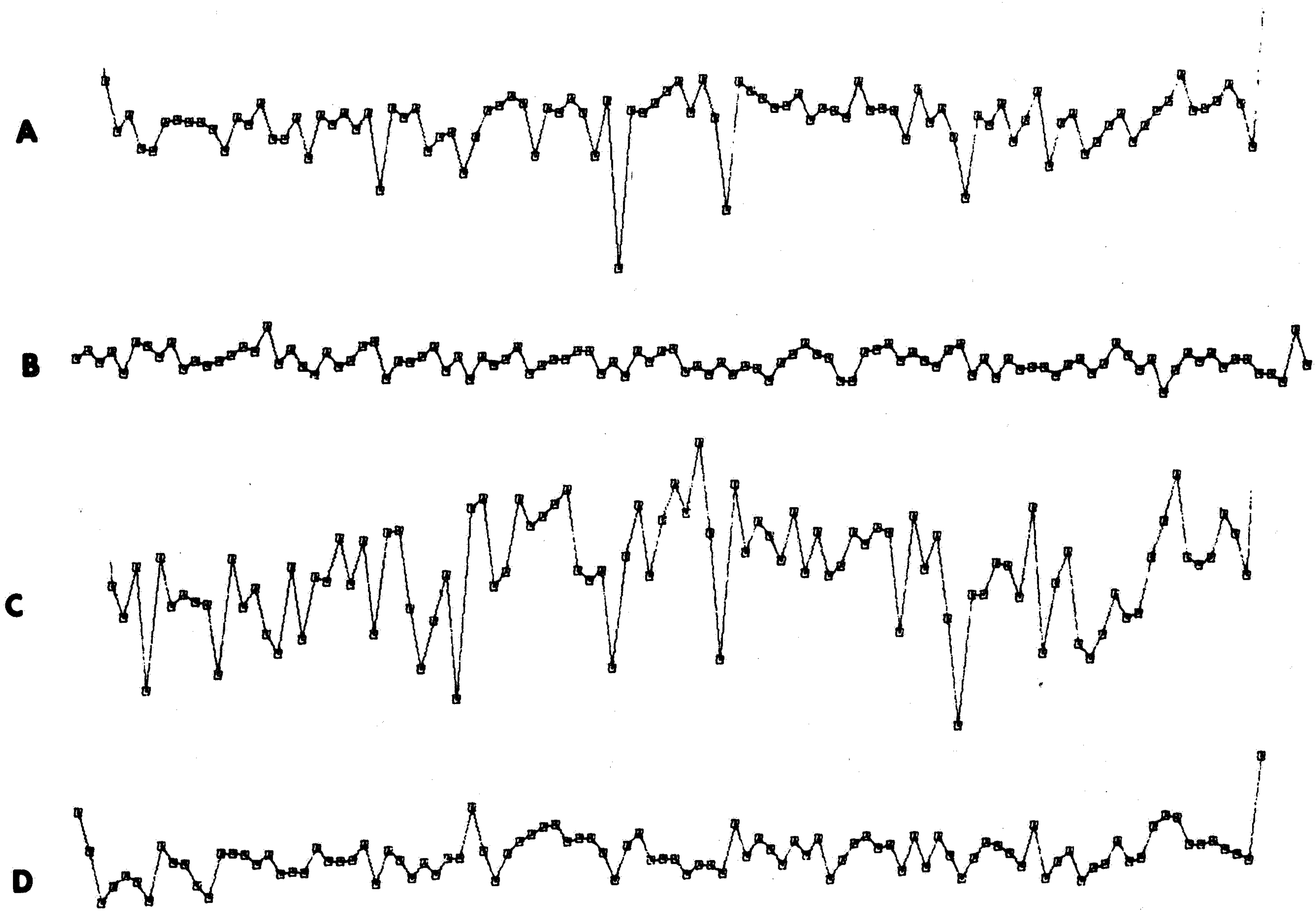

Figure 2. Computer plots of 100-pixel line of video: (a) raw, 24% full scale, (b) processed, 24% full scale, (c) raw, 84% full scale, (d) processed, 84% full scale

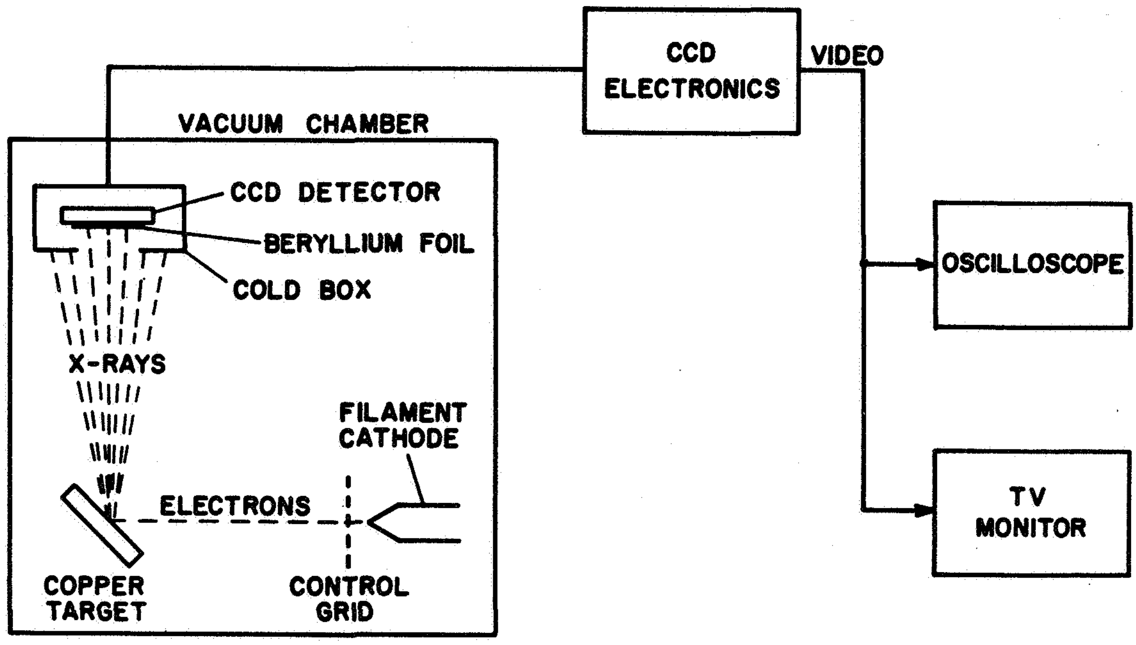

Figure 3. CCD x-ray experiment block diagram

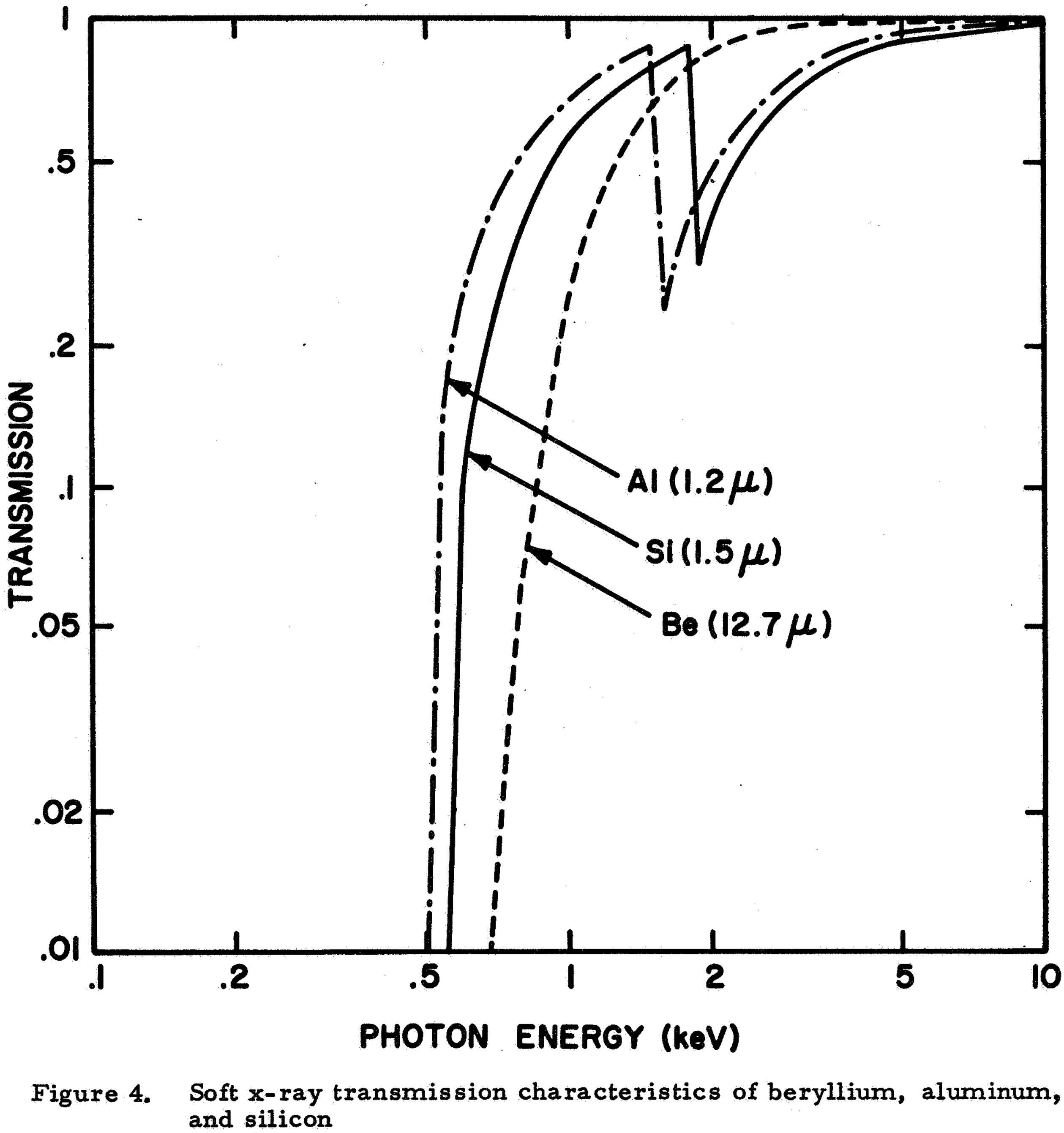

Figure 4. Soft x-ray transmission characteristics of beryllium, aluminum, and silicon

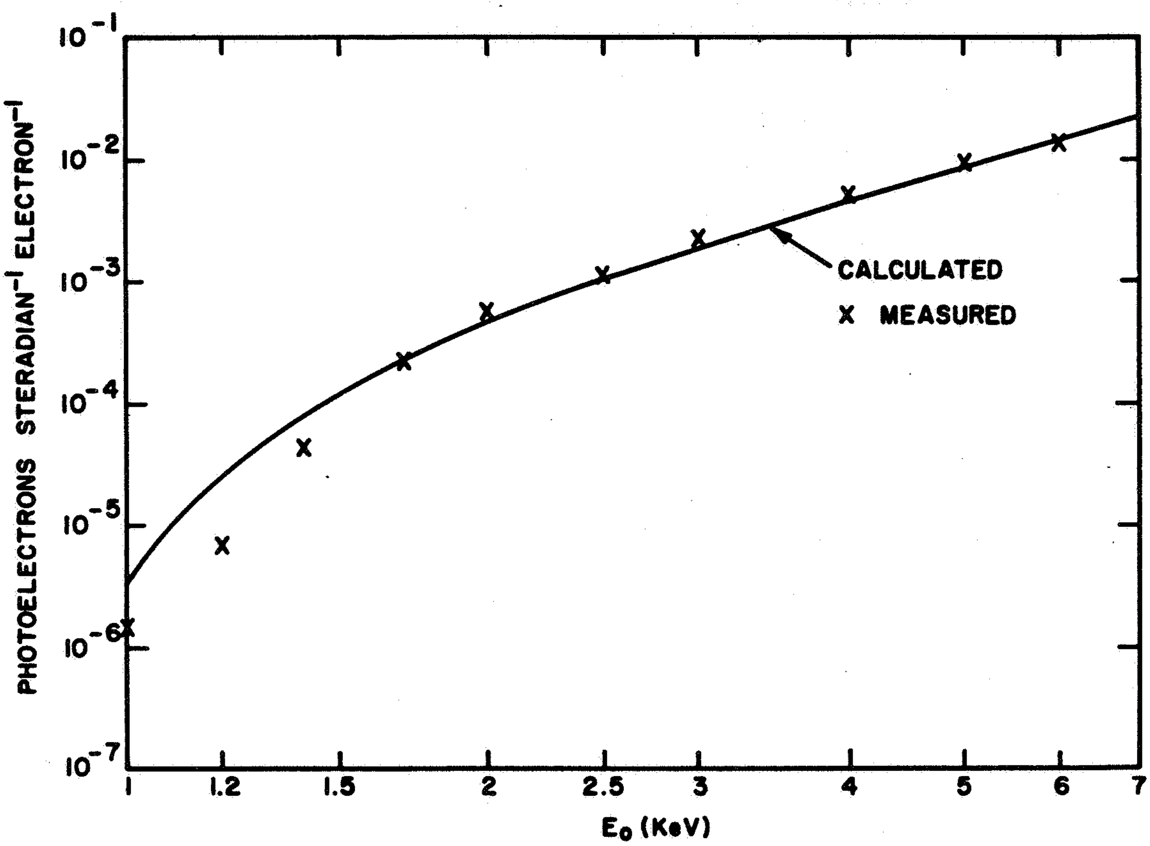

Figure 5. Fairchild CCD-201 response to soft x-rays, calculated and measured